Chapter 1
Nonlinear Vibrations of a Beam with a Breathing Edge Crack Using Multiple Trial Functions

Ali C. Batihan and Ender Cigeroglu

Abstract In this paper, a beam like structure with a single edge crack is modeled and analyzed in order to study the nonlinear effects of breathing crack on transverse vibrations of a beam. In literature, edge cracks are generally modeled as open cracks, in which the beam is separated into two pieces at the crack location and these pieces are connected to each other with a rotational spring to represent the effect of crack. The open edge crack model is a widely used assumption; however, it does not consider the nonlinear behavior due to opening and closing of the crack region. In this paper, partial differential equation of motion obtained by Euler-Bernoulli beam theory is converted into nonlinear ordinary differential equations by using Galerkin's method with multiple trial functions. The nonlinear behavior of the crack region is represented as a bilinear stiffness matrix. The nonlinear ordinary differential equations are converted into a set of nonlinear algebraic equations by using harmonic balance method (HBM) with multi harmonics. Under the action of a harmonic forcing, the effect of crack parameters on the vibrational behavior of the cracked beam is studied.

Keywords Breathing crack • Euler-Bernoulli beam • Galerkin's method • Harmonic balance method • Nonlinear vibrations

1.1 Introduction

Identification of cracks and determination of their location is an important consideration, since crack propagation may cause unexpected failure. Therefore, beams with edge cracks has been an interesting area of research. Dimarogonas [1] provides a review paper in which studies on open breathing crack, continuous crack beam theories and vibration of cracked plates are covered. Aydin [2], carried out a study considering arbitrary number of cracks and axial loads applied on a beam. Khiem and Lien [3], used a transfer matrix method in order to calculate natural frequencies of a beam with an arbitrary number of cracks. In order to see the effect of crack clearly, beam models with mass attachments are used by Mermertaş and Erol [4] and Zhong and Oyadiji [5]. Mazanoğlu et al. [6] applied Rayleigh-Ritz and finite element methods in order to study vibrations of non-uniform cracked beams. In a study of Chondros et al. [7], flexibility due to crack region is distributed along the whole beam by developing a continuous theory of cracked beams. In another study of Chondros et al. [8], breathing edge crack was studied by combining vibration characteristics of open and closed period as a bi-linear model. Cheng et al. [9] represented the breathing crack with time dependent stiffness. Finite element method was used by Chati et al. [10] in order to study modal analysis of a beam with a breathing edge crack. Giannini et al. [11] also used finite element method to identify sub and super harmonics of a beam with a breathing edge crack. Baeza and Ouyang [12], developed an analytical approach by using beam modes to calculate a scale factor matrix which indicates crack location.

In most of the studies available in literature, the beam is modeled by Euler-Bernoulli beam theory and the crack region is represented by a rotational spring whose stiffness is obtained by fracture mechanics methods. A significant number of studies are investigated the effect of crack parameters on natural frequencies. In addition, application of finite element methods for beams with breathing edge cracks is a common modeling approach.

In this paper, based on the previous study of authors [13], beam is modeled using Euler-Bernoulli beam theory and breathing edge crack is modeled as a piecewise linear stiffness. In the analytical model, the state of the crack is determined by checking the slope difference at the crack location. The governing equations are obtained by Galerkin's method utilizing multiple trial functions and the resulting set of nonlinear equations are solved by application of harmonic balance method with multi harmonics.

A.C. Batihan • E. Cigeroglu (✉)
Department of Mechanical Engineering, Middle East Technical University, Ankara 06800, Turkey
e-mail: ender@metu.edu.tr

G. Kerschen (ed.), *Nonlinear Dynamics, Volume 1*, Conference Proceedings of the Society for Experimental Mechanics Series,
DOI 10.1007/978-3-319-29739-2_1

1.2 Formulation of the Breathing Edge Crack Problem

Equation of motion of a uniform beam vibrating in transverse direction under the action of an external point force $f(t)$ located at L_f can expressed by utilizing Euler-Bernoulli beam theory as follows

$$EI\frac{\partial^4 w(x,t)}{\partial x^4} + c\frac{\partial w(x,t)}{\partial t} + m\frac{\partial^2 w(x,t)}{\partial t^2} = f(t)\delta\left(x - L_f\right), \tag{1.1}$$

where $w(x, t)$ is transverse displacement, EI is flexural rigidity, c is viscous damping coefficient and m is mass per unit length of the beam. Using expansion theorem, transverse displacement can be expressed as follows

$$w(x,t) = \sum_j a_j(t)\phi_j(x), \tag{1.2}$$

where $\phi_j(x)$ is the j^{th} mass normalized eigenfunction of a beam with an open edge crack and $a_j(t)$ is the corresponding modal coefficient. Substituting Eq. (1.2) into Eq. (1.1), the following expression is obtained

$$\sum_j \left(EIa_j(t)\frac{d^4\phi_j(x)}{dx^4}\right) + \sum_j \left(c\dot{a}_j(t)\phi_j(x)\right) + \sum_j \left(m\ddot{a}_j(t)\phi_j(x)\right) = f(t)\delta\left(x - L_f\right). \tag{1.3}$$

Multiplying Eq. (1.3) by $\phi_i(x)$ and integrating over the spatial domain of the beam result in the following equation

$$\sum_j \left(k_{ij}\right) a_j(t) + \sum_j \left(c_{ij}\right)\dot{a}_j(t) + \sum_j \left(m_{ij}\right)\ddot{a}_j(t) = F_i(t), \tag{1.4}$$

where

$$k_{ij} = \int_0^L EI\phi_i(x)\frac{d^4\phi_j(x)}{dx^4}dx, \tag{1.5}$$

$$c_{ij} = \int_0^L c\phi_i(x)\phi_j(x)dx, \tag{1.6}$$

$$m_{ij} = \int_0^L m\phi_i(x)\phi_j(x)dx, \tag{1.7}$$

$$F_i(t) = \phi_i\left(L_f\right)f(t). \tag{1.8}$$

Equation (1.4) can be rearranged as a matrix equation as follows

$$[M]\{\ddot{a}\} + [C]\left\{\dot{a}\right\} + [K]\{a\} = \{F\}, \tag{1.9}$$

where $[M]$, $[C]$ and $[K]$ are the corresponding mass, damping and stiffness matrices of a beam with an open edge crack.

Figure 1.1 shows the deformed shape of a cantilever crack beam at two different time instants. During vibration, due to breathing effect of the edge crack, the beam behaves as if it is an undamaged beam for some period of cycle; whereas, in the rest of the cycle it behaves as a beam with an open edge crack. Therefore, beam with a breathing edge crack can be represented as a combination of two linear systems as shown in Fig. 1.1.

In order to consider the breathing effect, two different sets of mass normalized eigenfunctions are utilized as trial functions. For the time instant when the crack is closed, mass, damping and stiffness matrices are calculated by utilizing first few mass normalized eigenfunctions of the undamaged beam; whereas mass normalized eigenfunctions of a beam with an open crack are used in case the crack is in open state. The details and derivation of these eigenfunctions can be found in [14]. As the

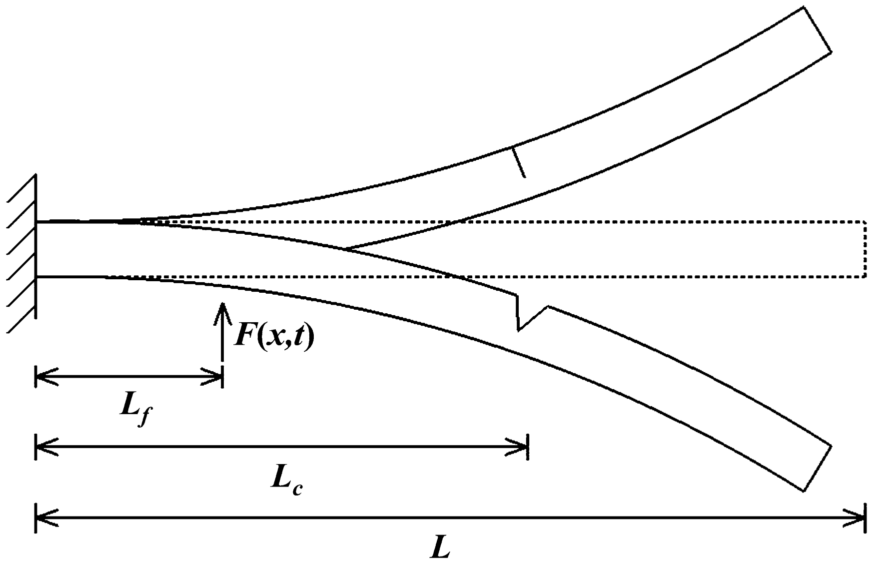

Fig. 1.1 Cantilever beam with a breathing edge crack

crack switches from open state to closed state, mass and damping matrices remain unchanged; however, the stiffness matrix increases when the crack closes. The increase in the stiffness matrix is given by the following relation

$$[B] = [K_c] - [K], \tag{1.10}$$

where $[K_c]$ is the stiffness matrix of the beam when the crack is at the closed state.

In this study, in order to identify whether the crack is open or not, the slope difference at the crack location is checked. Negative slope difference states that the crack is open and the nonlinear forcing term is zero; whereas positive slope difference indicates that the crack is closed and the nonlinear forcing term is nonzero. The periodic change in the stiffness of the beam which results from the breathing effect of the crack, leads to the following nonlinear forcing term

$$\{R(\{a\})\} = \begin{cases} [B]\{a\} & if \ \left.\frac{\partial w(x,t)}{\partial x}\right|_{x=L_c} \geq 0 \\ \{0\} & if \ \left.\frac{\partial w(x,t)}{\partial x}\right|_{x=L_c} < 0 \end{cases}. \tag{1.11}$$

Adding the nonlinear forcing term $\{R(\{a\})\}$, into Eq. (1.9) leads to the following equation in which the breathing effect of the crack is taken into consideration

$$[M]\{\ddot{a}\} + [C]\{\dot{a}\} + [K]\{a\} + \{R(\{a\})\} = \{F\}. \tag{1.12}$$

1.3 Harmonic Balance Method

In order to utilize harmonic balance method with multi harmonics, modal coefficient of each trial function is expressed as follows

$$a_j(t) = a_{j0} + \sum_p a_{jcp}\cos(p\omega t) + \sum_p a_{jsp}\sin(p\omega t), \tag{1.13}$$

where a_{j0} is the bias term of the j^{th} modal coefficient, a_{jcp} and a_{jsp} are the coefficients of cosine and sine components of the p^{th} harmonic of the j^{th} modal coefficient. Letting $\theta = \omega t$ and rearranging Eq. (1.13), the modal coefficients can be written in vector form as

$$\{a\} = \{a_0\} + [a_c]\{h_c(\theta)\} + [a_s]\{h_c(\theta)\}, \tag{1.14}$$

where

$$[a_c] = \left[\{a_{c1}\} \cdots \{a_{cp}\}\right], \tag{1.15}$$

$$[a_s] = \left[\{a_{s1}\} \cdots \{a_{sp}\}\right], \tag{1.16}$$

and $\{h_c(\theta)\}$ & $\{h_s(\theta)\}$ are the following vectors whose lengths are equal to the number harmonics (p) used

$$\{h_c(\theta)\} = \left\{\begin{array}{c} \cos(\theta) \\ \vdots \\ \cos(p\theta) \end{array}\right\}, \tag{1.17}$$

$$\{h_s(\theta)\} = \left\{\begin{array}{c} \sin(\theta) \\ \vdots \\ \sin(p\theta) \end{array}\right\}. \tag{1.18}$$

The periodic nonlinear forcing term $\{R(\{a\})\}$ can be expressed by Fourier series as

$$\{R\} = \frac{1}{2}\{R_0\} + [R_c]\{h_c(\theta)\} + [R_s]\{h_s(\theta)\}. \tag{1.19}$$

where

$$[R_c] = \left[\{R_{c1}\} \cdots \{R_{cp}\}\right], \tag{1.20}$$

$$[R_s] = \left[\{R_{s1}\} \cdots \{R_{sp}\}\right], \tag{1.21}$$

and

$$R_{j0} = \frac{1}{\pi}\int_0^{2\pi} R_j(\theta)\, d\theta, \tag{1.22}$$

$$R_{jcp} = \frac{1}{\pi}\int_0^{2\pi} R_j(\theta)\cos(p\theta)\, d\theta, \tag{1.23}$$

$$R_{jsp} = \frac{1}{2\pi}\int_0^{2\pi} R_j(\theta)\sin(p\theta)\, d\theta. \tag{1.24}$$

Similarly external forcing, $f(t)$ can be represented by Fourier series as follows

$$f(t) = \{f_{cp}\}'\{h_c(\theta)\} + \{f_{sp}\}'\{h_s(\theta)\}. \tag{1.25}$$

Substituting Eqs. (1.14), (1.19) and (1.25) into Eq. (1.12) and collecting sine and cosine terms leads to the following set of nonlinear equations

$$\begin{aligned}&\left(\begin{bmatrix}[K] & & 0\\ & \ddots & \\ 0 & & [K]\end{bmatrix} - \omega^2\begin{bmatrix}[M] & & 0\\ & \ddots & \\ 0 & & [M]\end{bmatrix}\begin{bmatrix}[I] & & \\ & \ddots & \\ & & p^2\,[I]\end{bmatrix}\right)\begin{Bmatrix}\{a_{c1}\}\\ \vdots \\ \{a_{cp}\}\end{Bmatrix} + \begin{Bmatrix}\{R_{c1}\}\\ \vdots \\ \{R_{cp}\}\end{Bmatrix}\\ &+\omega\begin{bmatrix}[C] & & 0\\ & \ddots & \\ 0 & & [C]\end{bmatrix}\begin{bmatrix}[I] & & \\ & \ddots & \\ & & p\,[I]\end{bmatrix}\begin{Bmatrix}\{a_{s1}\}\\ \vdots \\ \{a_{sp}\}\end{Bmatrix} - \begin{bmatrix}\left[\phi_{L_f}\right] & & 0\\ & \ddots & \\ 0 & & \left[\phi_{L_f}\right]\end{bmatrix}\begin{Bmatrix}f_{c1}\,\{I\}\\ \vdots \\ f_{cp}\,\{I\}\end{Bmatrix} = \begin{Bmatrix}\{0\}\\ \vdots \\ \{0\}\end{Bmatrix},\end{aligned} \tag{1.26}$$

$$\begin{aligned}&\left(\begin{bmatrix}[K] & & 0\\ & \ddots & \\ 0 & & [K]\end{bmatrix} - \omega^2\begin{bmatrix}[M] & & 0\\ & \ddots & \\ 0 & & [M]\end{bmatrix}\begin{bmatrix}[I] & & \\ & \ddots & \\ & & p^2\,[I]\end{bmatrix}\right)\begin{Bmatrix}\{a_{s1}\}\\ \vdots \\ \{a_{sp}\}\end{Bmatrix} + \begin{Bmatrix}\{R_{s1}\}\\ \vdots \\ \{R_{sp}\}\end{Bmatrix}\\ &+\omega\begin{bmatrix}[C] & & 0\\ & \ddots & \\ 0 & & [C]\end{bmatrix}\begin{bmatrix}[I] & & \\ & \ddots & \\ & & p\,[I]\end{bmatrix}\begin{Bmatrix}\{a_{c1}\}\\ \vdots \\ \{a_{cp}\}\end{Bmatrix} - \begin{bmatrix}\left[\phi_{L_f}\right] & & 0\\ & \ddots & \\ 0 & & \left[\phi_{L_f}\right]\end{bmatrix}\begin{Bmatrix}f_{s1}\,\{I\}\\ \vdots \\ f_{sp}\,\{I\}\end{Bmatrix} = \begin{Bmatrix}\{0\}\\ \vdots \\ \{0\}\end{Bmatrix},\end{aligned} \tag{1.27}$$

$$[K]\,\{a_0\} + \frac{1}{2}\,\{R_0\} = \{0\}\,, \tag{1.28}$$

where $[I]$ is the identity matrix, $\{I\}$ is a vector elements of which are all 1, and

$$\left[\phi_{L_f}\right] = \begin{bmatrix}\phi_1\left(L_f\right) & & 0\\ & \ddots & \\ 0 & & \phi_j\left(L_f\right)\end{bmatrix}. \tag{1.29}$$

1.4 Case Study and Discussion

Effect of breathing edge crack for different crack parameters is studied by using a cantilever beam model with the following properties: $L = 1$ m, $I = 2.667 \cdot 10^{-8}$ m^4, $\rho = 7850$ kg/m^3, $A = 8 \cdot 10^{-4}$ m^2, $E = 206$ GPa, $\zeta = 0.07$, $L_f = 0.1$ m and $f(t) = 100\cos(\omega t)$ N. Galerkin's method is applied by utilizing first three modes of the beam and the resulting set of nonlinear ordinary differential equations are converted into a set of nonlinear algebraic equations by using harmonic balance method with multi harmonics. According to [13], as crack ratio increases fundamental frequency decreases. Similarly, crack location also affects the fundamental frequency depending on the boundary conditions of the beam. The effect of different crack ratio and crack location on natural frequencies is given in Fig. 1.2. It is observed from the results that the effect of crack parameters on natural frequencies are not significant. Therefore, alternative features should be considered in crack detection problems.

In Fig. 1.3, absolute value of bias term of each modal coefficient as function of frequency is given. It is observed that bias term of each modal coefficient is influenced by both crack location and crack ratio. In Fig. 1.3a, bias term of each modal coefficient is plotted for different crack locations and it is observed that depending on the crack location bias term of different modal coefficient becomes dominant. Bias terms are also affected by the crack ratio, however the effect of crack ratio is not similar to the effect of crack location. For instance, from Fig. 1.3b it is observed that, an increase in crack depth shifts all the plots upward and the order of dominancy is conserved.

The amplitude of p^{th} harmonic of j^{th} modal coefficient is expressed by the following equation

$$a_{jp} = \sqrt{{a_{jcp}}^2 + {a_{sjp}}^2}. \tag{1.30}$$

In Fig. 1.4, amplitudes of the first harmonic of modal coefficients with respect to frequency are given for different crack location and ratio. From the plots, it is observed that first harmonics are slightly influenced by crack parameters. However, the first harmonic is the most dominant harmonic on the total response among the higher harmonics. This fact also explains why crack parameters have negligible effect on the total response.

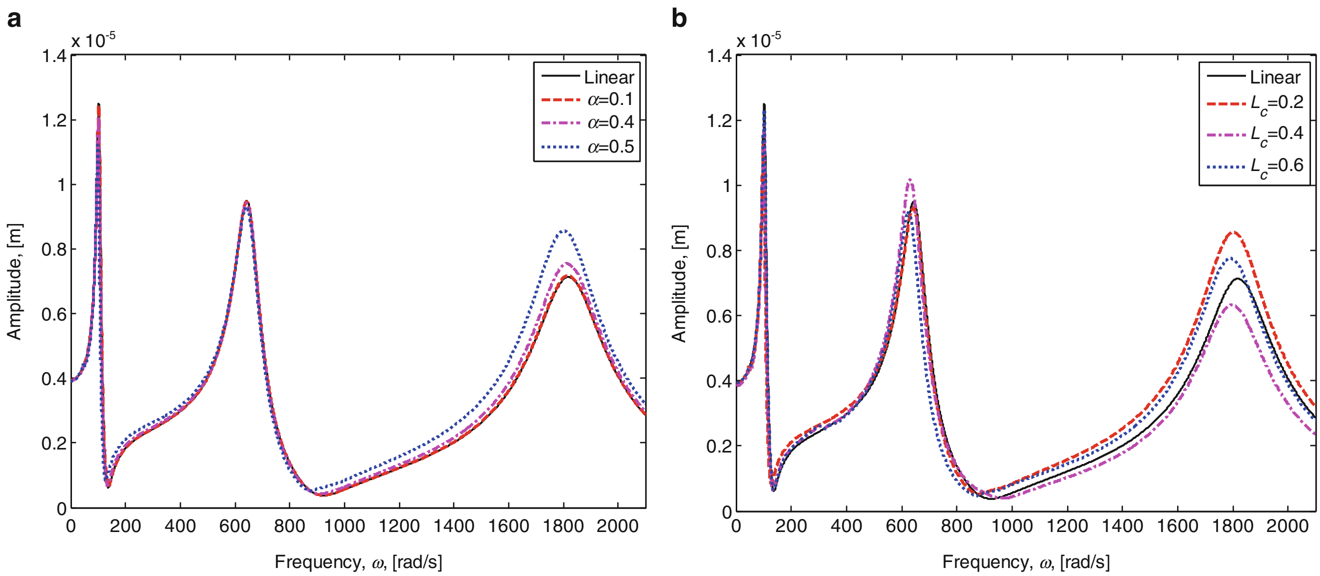

Fig. 1.2 Transverse displacement of a point at location $L_p = 0.1$ m vs. frequency. (**a**) For $L_c = 0.2$ m and different crack ratio. (**b**) For $\alpha = 0.5$ and different crack location

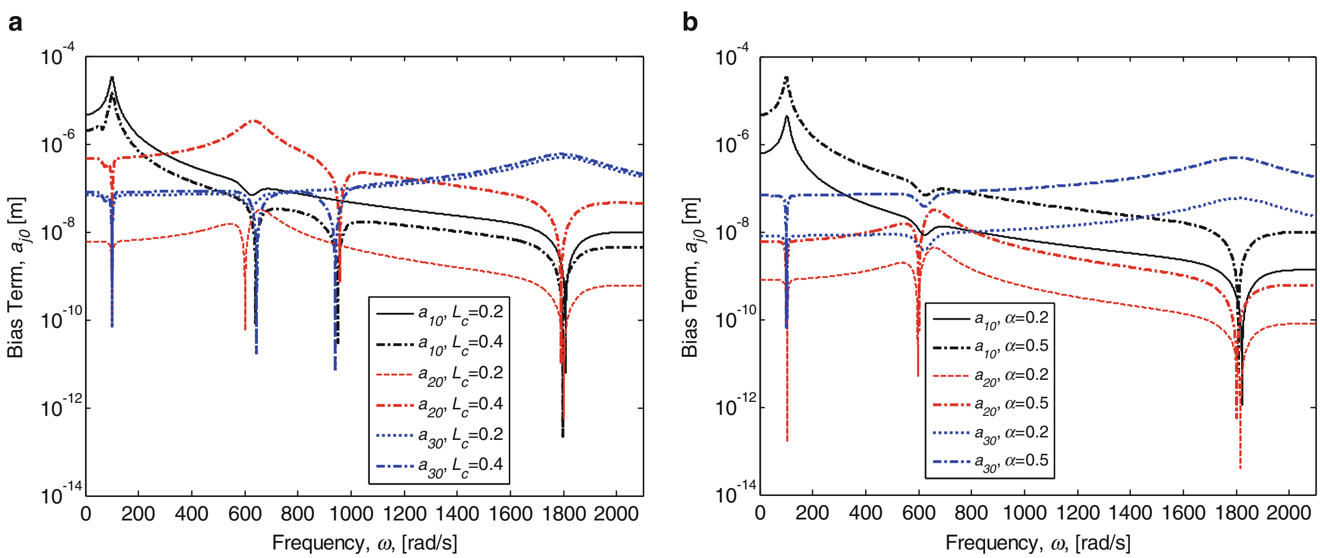

Fig. 1.3 Bias term of each modal coefficient vs. frequency. (**a**) For $\alpha = 0.5$ and different crack location. (**b**) For $L_c = 0.2$ m and different crack ratio

Higher harmonics of different trial functions for different crack parameters are shown in Figs. 1.5, 1.6, 1.7, and 1.8. Studying these figures, it is observed that higher harmonics can be grouped as even and odd harmonics depending on the similarities of the plots. Observing Figs. 1.5 and 1.6, it is seen that effect of crack parameters on even harmonics is similar to the effect of crack parameters on bias terms. As crack location changes, even harmonic of a different trial function becomes more dominant; whereas increase in crack depth causes an increase in the overall amplitude of the even harmonics.

Effect of crack parameters can also be observed in the odd harmonics. As depicted in Figs. 1.7 and 1.8, effect of crack location on odd harmonics is similar to the effect of crack location on bias terms and even harmonics. Studying the same figures, it is also observed that, odd harmonics of the first modal coefficient are significantly affected by crack depth. However, getting information from the odd harmonics of the second and the third modal coefficient is a more challenging due to scattered pattern. Therefore, analyzing the even harmonics can be used as means for crack detection problems. In Table 1.1,

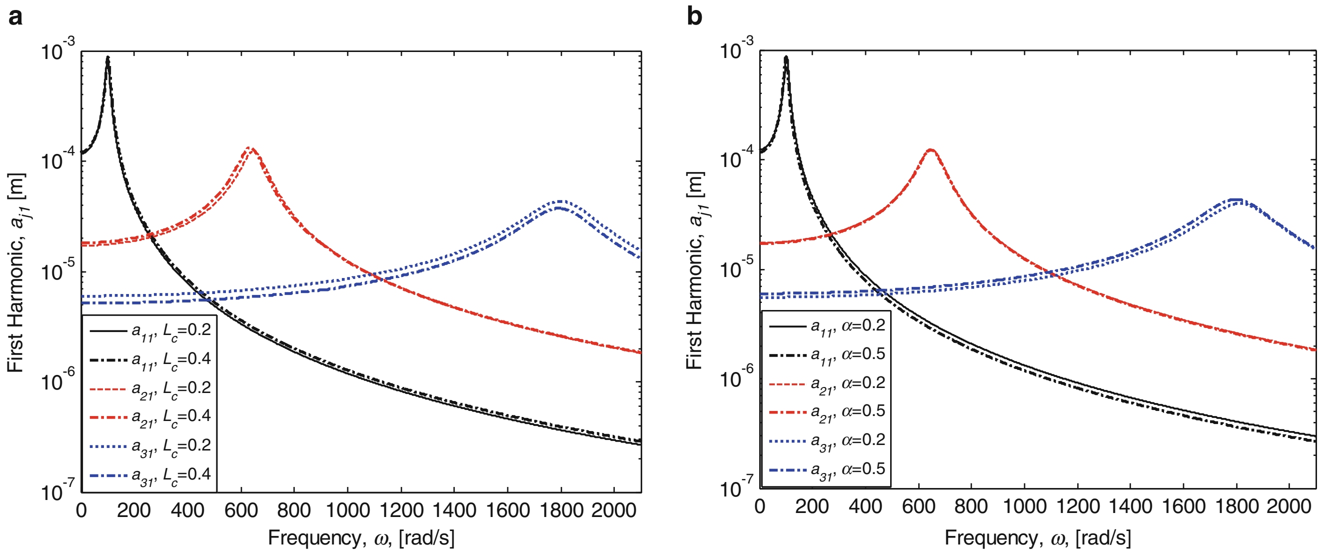

Fig. 1.4 First harmonic of each modal coefficient vs. frequency. (**a**) For $\alpha = 0.5$ and different crack location. (**b**) For $L_c = 0.2$ m and different crack ratio

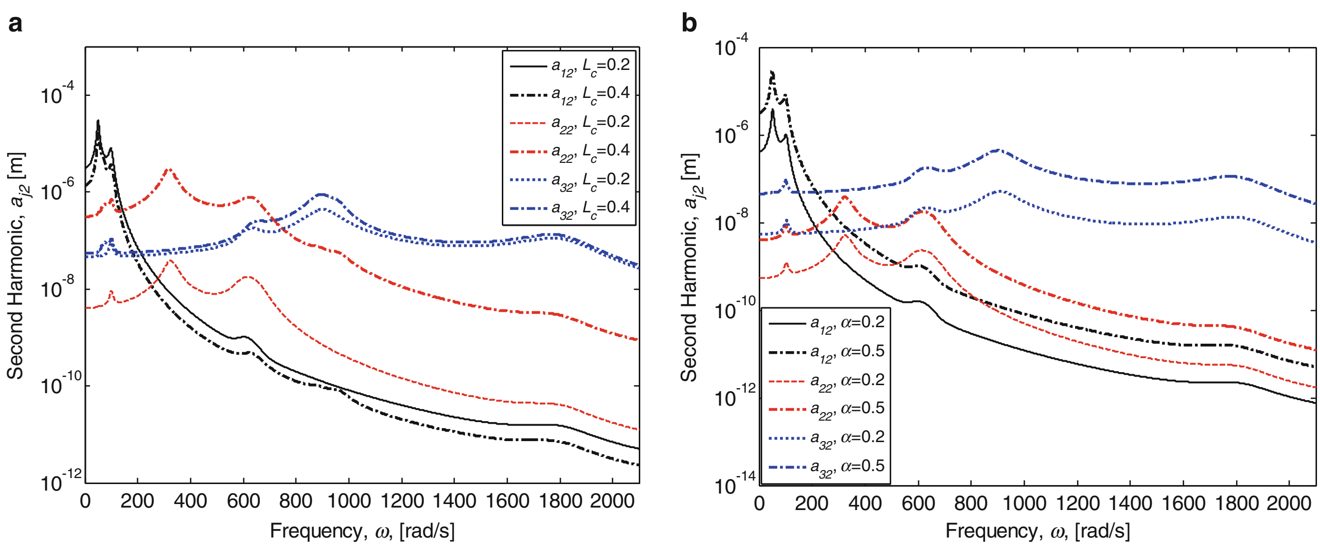

Fig. 1.5 Second harmonic of each modal coefficient vs. frequency. (**a**) For $\alpha = 0.5$ and different crack location. (**b**) For $L_c = 0.2$ m and different crack ratio

ratio of maximum amplitudes of the even harmonics are provided. The ratio is obtained by dividing maximum amplitude of p^{th} harmonic of each modal coefficient to the maximum amplitude of p^{th} harmonic of the first modal coefficient. Studying Table 1.1, significant effect of crack location on other trial functions can be observed.

In order to study the effect of crack depth on harmonics of different modal coefficients Table 1.2 is prepared in a similar way. In Figs. 1.5b and 1.6b it is observed that the increase in crack depth also increases all the plots with a similar magnitude. As a result of this fact, order of magnitude of the harmonics do not change. Therefore, in Table 1.2, it is observed that the maximum amplitude ratio is not influenced by the crack ratio.

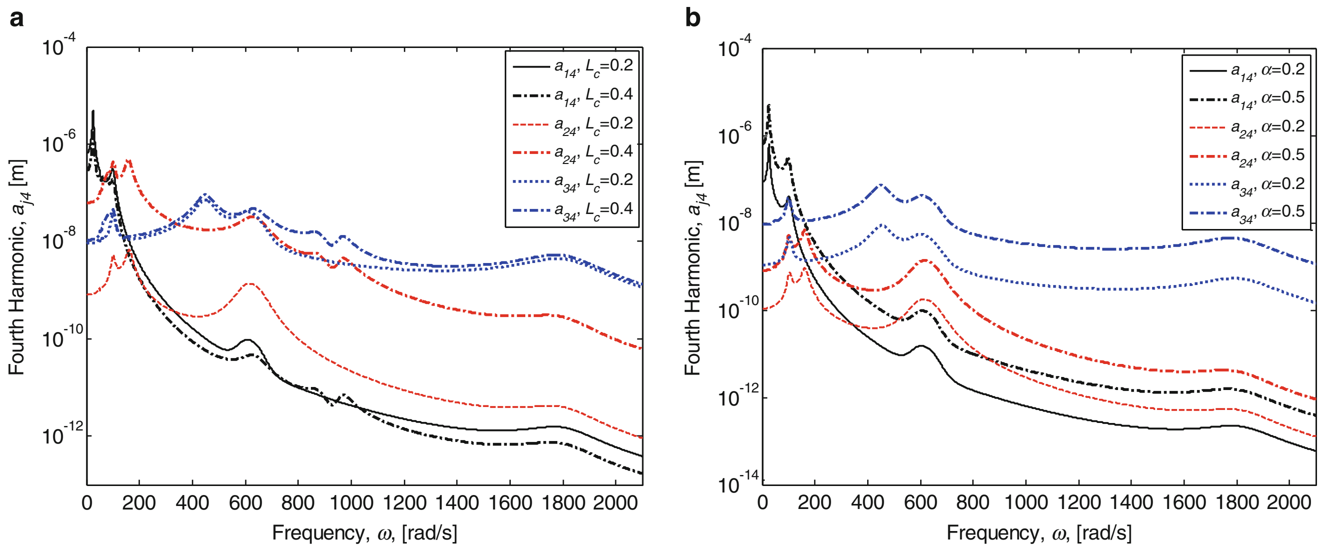

Fig. 1.6 Fourth harmonic of each modal coefficient vs. frequency. (**a**) For $\alpha = 0.5$ and different crack location. (**b**) For $L_c = 0.2$ m and different crack ratio

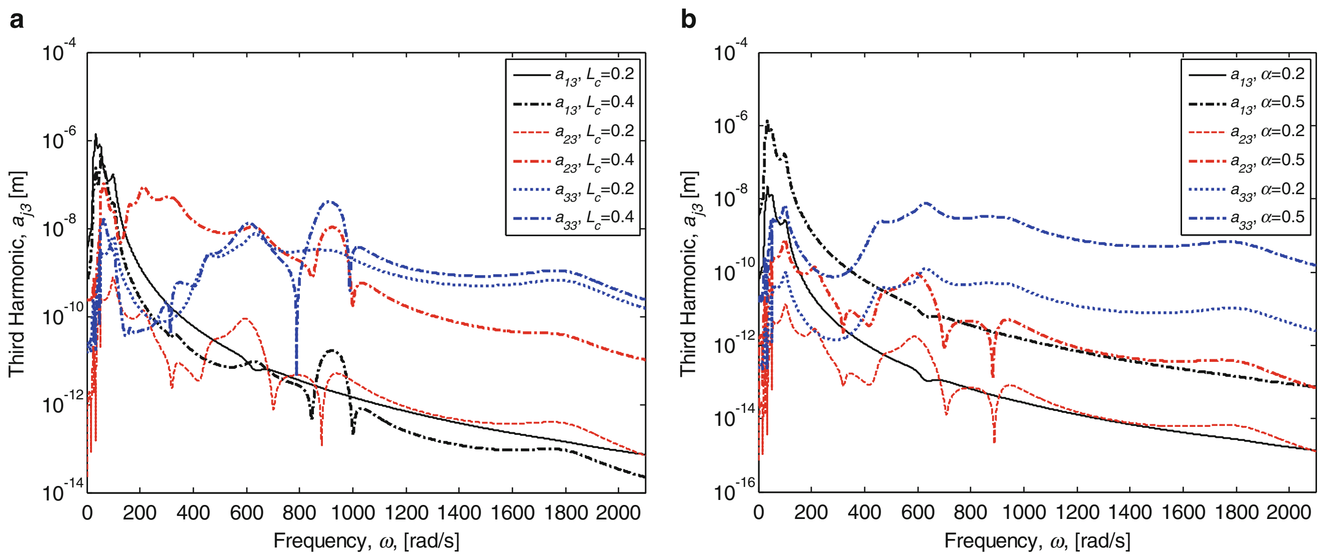

Fig. 1.7 Third harmonic of each modal coefficient vs. frequency. (**a**) For $\alpha = 0.5$ and different crack location. (**b**) For $L_c = 0.2$ m and different crack ratio

1.5 Conclusion

In this study, beam with breathing edge crack is modelled by using Euler-Bernoulli beam theory and nonlinear piecewise linear stiffness. Multiple trial functions are used to represent the response in Galerkin's method where a piecewise linear stiffness matrix based on the slope difference at the crack location is introduced. Harmonic Balance Method with multiple harmonics is used to convert nonlinear ordinary differential equation into a set of nonlinear algebraic equations. It is observed from the results that effect of crack parameters on the natural (resonance) frequency of the cracked beam is insignificant. However, it is observed that harmonics of the response are affected from the crack parameters significantly; hence, this information can be used for the crack detection. Both crack depth and crack location affects the amplitudes of the harmonics of each modal coefficient. As crack ratio increases the amplitudes of the harmonics also increase, however the order of magnitudes of the harmonics are not affected by the crack ratio. The crack location affects amplitudes of the harmonics as well as the order of magnitudes of the harmonics. Depending on the crack location, a harmonic of a different modal coefficient becomes dominant. This fact explains the necessity of using multiple trial functions.

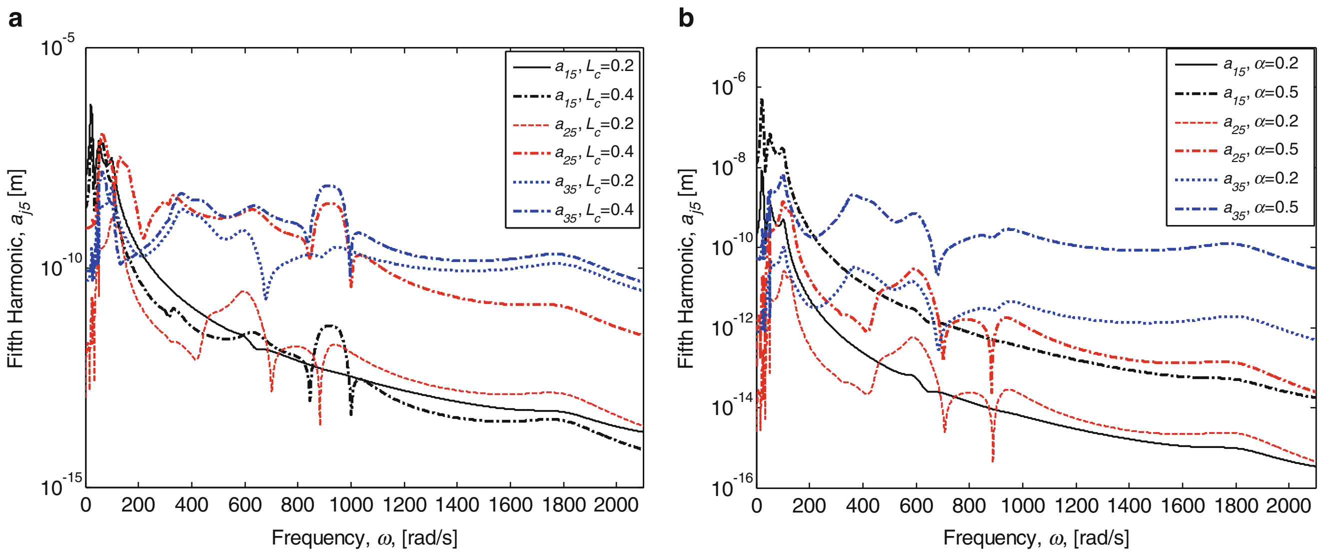

Fig. 1.8 Fifth harmonic of each modal coefficient vs. frequency. (**a**) For $\alpha = 0.5$ and different crack location. (**b**) For $L_c = 0.2$ m and different crack ratio

Table 1.1 Ratio of maximum amplitudes of even harmonics of each modal coefficient for different crack location

	$\alpha = 0.5$					
L_c	a_{12}/a_{12}	a_{22}/a_{12}	a_{32}/a_{12}	a_{14}/a_{14}	a_{24}/a_{14}	a_{34}/a_{14}
0.2	1	0.00128	0.01438	1	0.00141	0.0151
0.4	1	0.18786	0.05545	1	0.22663	0.04163

Table 1.2 Ratio of maximum amplitudes of even harmonics of each modal coefficient for different crack depth

	$L_c = 0.2$					
α	a_{12}/a_{12}	a_{22}/a_{12}	a_{32}/a_{12}	a_{14}/a_{14}	a_{24}/a_{14}	a_{34}/a_{14}
0.2	1	0.00132	0.01327	1	0.00147	0.01385
0.5	1	0.00128	0.01437	1	0.00141	0.01507

References

1. Dimarogonas, A.D.: Vibration of cracked structures: a state of the art review. Eng. Fract. Mech. **55**(5), 831–857 (1996)
2. Aydın, K.: Vibratory characteristics of Euler-Bernoulli beams with arbitrary number of cracks subjected to axial load. J. Vib. Control. **14**(4), 485–510 (2008)
3. Khiem, N.T., Lien, T.V.: A simplified method for natural frequency analysis of multiple cracked beam. J. Sound Vib. **254**(4), 737–751 (2001)
4. Mermertaş, V., Erol, H.: Effect of mass attachment on the free vibration of cracked beam. In: The 8th International Congress on Sound and Vibration (2001)
5. Zhong, S., Oyadiji, S.O.: Analytical predictions of natural frequencies of cracked simply supported beam with stationary roving mass. J. Sound Vib. **311**, 328–352 (2008)
6. Mazanoğlu, K., Yeşilyurt, I., Sabuncu, M.: Vibration analysis of multiple cracked non-uniform beams. J. Sound Vib. **320**, 977–989 (2009)
7. Chondros, T.G., Dimarogonas, A.D., Yao, J.: A continuous cracked beam vibration theory. J. Sound Vib. **215**(1), 17–34 (1998)
8. Chondros, T.G., Dimarogonas, A.D., Yao, J.: Vibration of a beam with a breathing crack. J. Sound Vib. **239**(1), 57–67 (2001)
9. Cheng, S.M., Wu, X.J., Wallace, W.: Vibrational response of a beam with a breathing crack. J. Sound Vib. **225**(1), 201–208 (1999)
10. Chati, M., Rand, R., Mukherjee, S.: Modal analysis of a cracked beam. J. Sound Vib. **207**(2), 249–270 (1997)
11. Giannini, O., Casini, P., Vestroni, F.: Nonlinear harmonic identification of breathing cracks in beams. Comput. Struct. **129**, 166–177 (2013)
12. Baeza, L., Ouyang, H.: Modal approach for forced vibration of beams with a breathing crack. Key Eng. Mater. **413–414**, 39–46 (2009)
13. Batihan, A.C., Cigeroglu, E.: Nonlinear vibrations of a beam with a breathing edge crack. In: IMAC XXXIII (2015)
14. Batihan, A.C.: Vibration analysis of cracked beams on elastic foundation using Timoshenko beam theory. Master Thesis, Middle East Technical University (2011)